

The mechanism for the long-wave instability in thin liquid films

By MARC K. SMITH

Department of Mechanical Engineering, The Johns Hopkins University,
Baltimore, MD 21218, USA

(Received 3 October 1988 and in revised form 25 January 1990)

A physical mechanism for the long-wave instability of thin liquid films is presented. We show that the many diverse systems that exhibit this instability can be classified into two large groups. Each group is studied using the model of a thin liquid film with a deformable top surface flowing down a rigid inclined plane. In the first group, the top surface has an imposed stress, while in the other, an imposed velocity. The proposed mechanism shows how the details of the energy transfer from the basic state to the disturbance are handled differently in each of these cases, and how a common growth mechanism produces the unstable motion of the disturbance.

1. Introduction

A large amount of research on the behaviour of thin liquid films has been done in the last half century because of the prevalence of such films in technologically important processes. Liquid films are used to remove heat from solid surfaces and they appear as condensate films on cold surfaces. In coating technology, the behaviour of the initial liquid film can affect the quality of the final coated surface. Thin films are also used as lubricant layers for the flow of crude oil in pipes and channels. The research on thin liquid films has investigated systems that are isothermal, that are heated or cooled, that are composed of several liquid layers with density and/or viscosity stratification, and films that are contained within pipes or channels. Driving forces include moving boundaries, gravity, applied pressure gradients, shear stresses, and thermocapillarity.

One interesting feature of thin liquid-film flows is the appearance of an instability in the form of a surface wave whose wavelength is much larger than the depth of the film. Since the instability can occur at very low values of the Reynolds number, it is important to understand it thoroughly. This long-wave instability has been examined both theoretically and experimentally by a large number of investigators. The pioneering theoretical work was done by Benjamin (1957) and Yih (1963, 1967), but Binnie (1957), Kao (1965*a, b*, 1968), Lin (1975), Akhtaruzzaman, Wang & Lin (1978), Wang, Seaborg & Lin (1978), Hickox (1971), Smith & Davis (1982), Joseph, Renardy & Renardy (1984), Goussis & Kelly (1985, 1988), Hooper (1985), Renardy (1987*a, b*), Lister (1987), Than, Rosso & Joseph (1987), Smith (1989), Kelly *et al.* (1989), and many others have made contributions to this problem.

The theoretical stability problem is particularly simple because one can use a regular perturbation expansion to obtain the critical Reynolds number. However, in spite of this simplicity, there has been very little discussion of the physical mechanism of the long-wave instability.

Yih (1967) states that the long-wave instability of an isothermal film flow on a

rigid inclined plane obtains its power from the longitudinal component of gravity. This is true, but what is the process through which gravity does work on the disturbance? What forces or flows are involved in creating the unstable motion of the interface? A mechanism which answers these questions would provide an understanding of this instability that could unify all the separate results that have been obtained to date.

Kelly *et al.* (1989) have provided one explanation for this mechanism by considering the flow of a single liquid film on a rigid inclined plane. The first part of their work was a disturbance energy analysis of the film flow for a disturbance of arbitrary wavelength. They identified the various contributions to the disturbance energy and found that when a film is unstable to long-wavelength disturbances, the disturbance energy increases because of the work done by a perturbation shear stress induced on the interface when it is displaced. They also presented a mechanism for the physical increase in the interfacial displacement of an unstable film by modifying the vorticity argument given by Hinch (1984) for the short-wave instability of an interface first studied by Hooper & Boyd (1983).

In the present work, we shall describe an alternative mechanism for the long-wave instability that does not invoke vorticity. This mechanism is composed of two parts; an initiating mechanism that drives the dominant motion in a perturbed film, and a growth mechanism that produces the unstable motion of the interface.

There are two different initiating mechanisms that can excite the long-wave interfacial instability in a thin film. We shall isolate these mechanisms by considering two model problems. The first is the familiar single liquid film flowing down a rigid inclined plane, bounded above by a gas. In this system, a tangential-stress boundary condition is imposed on the interface. For reasons which will become clear in the next section, we shall refer to the resultant long-wave instability as stress-induced. The second model is also a single liquid film flowing down a rigid inclined plane, but bounded above by a moving compliant surface (a thin elastic plate). Here, a tangential-velocity boundary condition is imposed on the interface and the resultant long-wave instability is velocity-induced. This distinction between the two different types of long-wave instability that are possible in isothermal liquid films has also been noted by Goussis & Kelly (1988).

The growth mechanism to be described is very general in that it outlines the proper sequence of events for the instability to occur in both of these models, even though the details of how the initial motion is induced are quite different. The mechanism also gives us a means to approximate the critical Reynolds number for these flows without having to solve the complete eigenvalue problem.

In §2, we shall consider the model for the stress-induced instability and briefly present the essential results of the long-wave stability calculation. The physical mechanism will then be described and we shall show how the mathematical analysis supports this mechanism. In §3, we shall do the same for the model of the velocity-induced instability. A more general discussion of the instability mechanism for both of these film flows is presented in §4, along with a simplified model of the instability. Finally, in §5, we state our conclusions and suggest further extensions to the mechanism.

2. Stress-induced instability

The simplest fluid system that exhibits the stress-induced instability is an isothermal liquid film of uniform depth h , density ρ , and dynamic viscosity μ , flowing

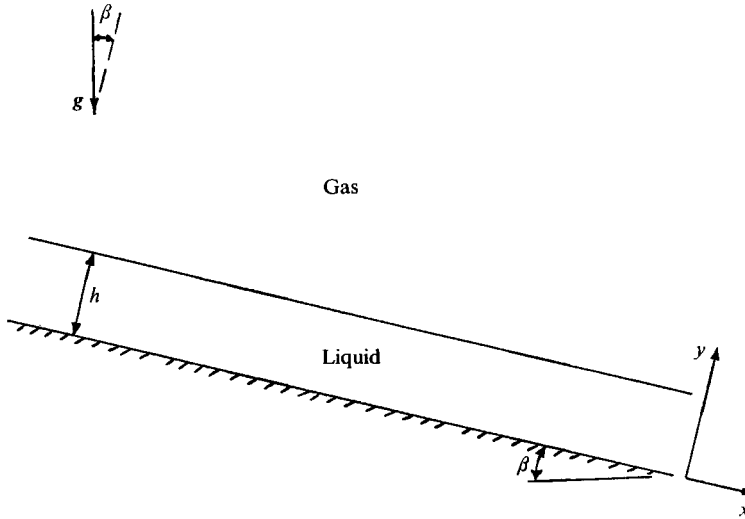


FIGURE 1. The geometry of the liquid film on a rigid inclined plane. The top surface is either a free surface with an imposed stress or a compliant surface with an imposed velocity.

down a rigid plane that is inclined at the angle β with respect to the horizontal. The film is bounded above by a gas which exerts a shear stress τ_t on the interface. This geometry is shown in figure 1. The stability of the free film with $\tau_t = 0$ was first studied theoretically by Benjamin (1957) and Yih (1963), while Smith & Davis (1982) included the non-zero surface stress to model the wind stress of the overlying gas.

The characteristic scales for the velocity, length, time, and pressure are $U_s = \rho gh^2 \sin(\beta)/\mu$, h , h/U_s , and $\mu U_s/h$ respectively. These scalings produce the following dimensionless groups: the Reynolds number $R = \rho^2 gh^3 \sin(\beta)/\mu^2$, the capillary number $Ca = \rho gh^2 \sin(\beta)/\sigma$, and the dimensionless surface stress $\tau = \tau_t/\rho gh \sin(\beta)$.

The basic state in this system is a steady, parallel shear flow driven by gravity and the applied shear stress. It is written in dimensionless form as

$$\bar{u} = (1 + \tau)y - \frac{1}{2}y^2, \quad \bar{p} = \cot(\beta)(1 - y), \tag{2.1 a, b}$$

$$\bar{v} = 0, \quad \bar{\eta} = 1. \tag{2.1 c, d}$$

The stability of this flow is examined using a standard linear stability analysis. The resulting two-dimensional, normal-mode disturbance equations are

$$R\{i\alpha(\bar{u} - c)\hat{u} + \bar{u}'\hat{v}\} = -i\alpha\hat{p} + D^2\hat{u} - \alpha^2\hat{u}, \tag{2.2 a}$$

$$i\alpha R(\bar{u} - c)\hat{v} = -D\hat{p} + D^2\hat{v} - \alpha^2\hat{v}, \tag{2.2 b}$$

$$D\hat{v} + i\alpha\hat{u} = 0, \tag{2.2 c}$$

$$\hat{u} = \hat{v} = 0 \quad \text{on } y = 0, \tag{2.2 d}$$

$$\hat{v} = i\alpha(\bar{u}(1) - c)\hat{\eta}, \quad D\hat{u} + i\alpha\hat{v} = -\bar{u}''(1)\hat{\eta} \quad \text{on } y = 1 \tag{2.2 e, f}$$

$$-\hat{p} + 2D\hat{v} = -\cot(\beta)\hat{\eta} + 2i\alpha\bar{u}'(1)\hat{\eta} - Ca^{-1}\alpha^2\hat{\eta} \quad \text{on } y = 1. \tag{2.2 g}$$

Here, $D^j = d^j/dy^j$ for $j = 1, 2$, α is the wavenumber of the disturbance, and $c = c_r + ic_i$ is a complex eigenvalue with c_r the phase speed and αc_i the growth rate of the instability.

The mechanism for the long-wave instability of this system can be seen in the

ordered problems that arise when the above eigenvalue problem is examined using a regular perturbation expansion for $\alpha \rightarrow 0$. Yih (1963) was the first to apply this technique to this problem, although he used the equivalent streamfunction formulation of the normal-mode equations. Using the long-wave expansions

$$\hat{u} = u_0 + \alpha u_1 + \alpha^2 u_2 + \dots, \quad (2.3a)$$

$$\hat{v} = \alpha v_1 + \alpha^2 v_2 + \dots, \quad (2.3b)$$

$$\hat{p} = p_0 + \alpha p_1 + \alpha^2 p_2 + \dots, \quad (2.3c)$$

$$\hat{\eta} = \eta_0 + \alpha \eta_1 + \alpha^2 \eta_2 + \dots, \quad (2.3d)$$

$$c = c_0 + \alpha c_1 + \alpha^2 c_2 + \dots, \quad (2.3e)$$

and the normalization $\eta_0 = 1$, $\eta_j = 0$, $j = 1, 2, 3, \dots$, we obtain the following ordered problems and their solutions. At $O(1)$,

$$D^2 u_0 = 0, \quad u_0(0) = 0, \quad Du_0(1) = 1, \quad (2.4a, b, c)$$

$$u_0(y) = y, \quad (2.4d)$$

$$Dp_0 = 0, \quad p_0(1) = \cot(\beta), \quad (2.5a, b)$$

$$p_0(y) = \cot(\beta). \quad (2.5c)$$

At $O(\alpha)$,

$$Dv_1 + iu_0 = 0, \quad v_1(0) = 0, \quad c_0 = \bar{u}(1) + iv_1(1), \quad (2.6a, b, c)$$

$$v_1(y) = -i\frac{1}{2}y^2, \quad c_0 = 1 + \tau. \quad (2.6d, e)$$

$$D^2 u_1 = ip_0 + iR(\bar{u} - c_0)u_0 + R\bar{u}'v_1, \quad (2.7a)$$

$$u_1(0) = 0, \quad Du_1(1) = 0, \quad (2.7b, c)$$

$$u_1(y) = i \cot(\beta) \left\{ \frac{1}{2}y^2 - y \right\} + iRc_0 \left\{ \frac{1}{24}y^4 - \frac{1}{6}y^3 + \frac{1}{3}y \right\}. \quad (2.7d)$$

And at $O(\alpha^2)$,

$$Dv_2 + iu_1 = 0, \quad v_2(0) = 0, \quad c_1 = iv_2(1), \quad (2.8a, b, c)$$

$$v_2(y) = \cot(\beta) \left\{ \frac{1}{6}y^3 - \frac{1}{2}y^2 \right\} + Rc_0 \left\{ \frac{1}{120}y^5 - \frac{1}{24}y^4 + \frac{1}{6}y^2 \right\}, \quad (2.8d)$$

$$c_1 = i \left\{ -\frac{1}{3} \cot(\beta) + \frac{2}{15} Rc_0 \right\}. \quad (2.8e)$$

Setting $c_i = 0$, we obtain the critical Reynolds number

$$R_c = \frac{5 \cot(\beta)}{2(1 + \tau)}. \quad (2.9)$$

This is the result of Smith & Davis (1982) for a film with a non-zero wind stress. It is also the result obtained by Benjamin (1957) and Yih (1963) for $\tau = 0$ when the difference in the velocity scale is considered. Note that the flow has a long-wave instability only when the phase speed of the disturbance is not contained in the range of \bar{u} .

For simplicity in the following discussion, we shall set $\tau = 0$ and discuss the physical mechanism of the long-wave instability in terms of the free film. However, the ideas we shall present are equally applicable to the more general case of a non-zero surface shear stress.

The initiating mechanism can be seen with the help of figure 2. Consider a sinusoidal disturbance to the free surface, η' . When the interface is deflected upward, the basic state has a shear stress at the new interface position because of the

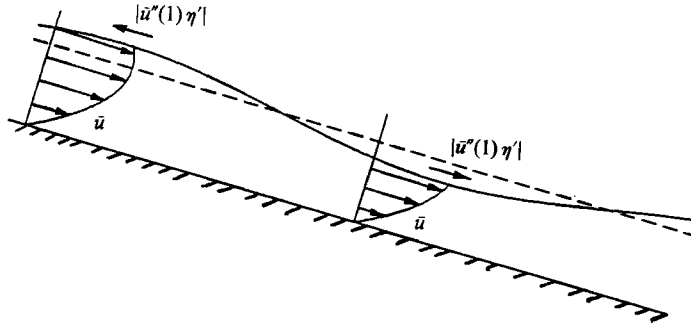


FIGURE 2. The development of an interfacial perturbation shear stress due to a disturbance on a free-surface film.

curvature of the velocity profile. This shear stress acts in the x -direction and it is equal to $\bar{u}''(1)\eta'$. Since the interface is a stress-free surface, a perturbation shear stress develops at the undisturbed interface position that exactly cancels the stress due to the basic state; see (2.2*f*). This perturbation shear stress drives a longitudinal flow underneath the disturbance crest that is linear and varies directly with the displacement of the interface as shown in figure 3 and equation (2.4*d*). This longitudinal shear flow is the dominant motion in the disturbed film and it is the end result of this initiating mechanism. Since it is driven at the interface, the energy for the flow comes from the work done by the perturbation surface shear stress. This is, and will remain, the dominant source of energy for the disturbance. To leading order, it is exactly balanced by viscous dissipation in the film. These observations agree completely with the disturbance energy analysis for this flow done by Kelly *et al.* (1989). These authors also described this initiating mechanism in much the same way.

The leading-order disturbance shear flow, shown in figure 3, is predominantly a parallel flow because the wavelength of the disturbance is large compared to the depth of the film. Its maximum amplitude occurs at the point of the maximum surface deflection. At the two node points, the deflection and the shear flow are both zero. In figure 4, we show a control volume enclosing the film on the right-hand side of a disturbance crest. There is a net inflow on the left-hand side of the control volume, but no outflow on the right-hand side. To conserve mass, the interface must be deflected in the positive y -direction. Likewise, for a control volume on the left-hand side of the crest, the interface must move in the $-y$ -direction. The net result of this behaviour is a wave motion of the disturbance to the right. The phase speed relative to the surface speed is related to the normal-mode volume flux of the disturbance by

$$c_0 - \bar{u}(1) = \int_0^1 u_0 dy = \frac{1}{2}.$$

Since $\bar{u}(1) = \frac{1}{2}$, $c_0 = 1$. Note that the maximum velocity of the film is at the free surface and so the disturbance moves faster than any fluid particle in the film.

The remaining leading-order effect of the disturbance is an increase in the hydrostatic pressure in the liquid under an interfacial elevation that is directly proportional to the component of gravity normal to the film, $\cot(\beta)$, and to the displacement of the interface; see (2.5*c*).

The growth mechanism of the instability uses the energy contained in the leading-

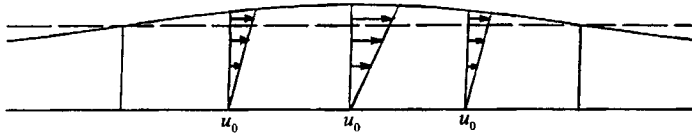


FIGURE 3. The leading-order longitudinal flow perturbation in the film. The long-dash line is the undisturbed free-surface position.

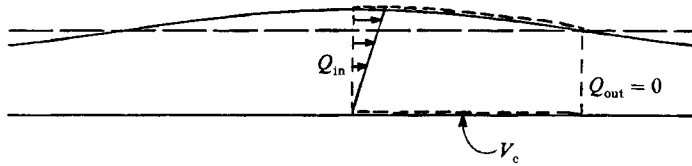


FIGURE 4. A disturbance to the free surface. The short-dash line on the right-hand side of the crest is the control volume V_c . The disturbance velocity profile on the left-hand side of the control volume is linear. There is no disturbance outflow. The long-dash line is the undisturbed free-surface position.

order shear flow to produce the unstable growth of the interfacial displacement. System (2.7a-c) is the key to this mechanism. It describes a shear flow in a film with one rigid and one free surface driven by the pressure and the inertial stresses from the leading-order disturbance flow. We can understand this flow by considering the simpler problem,

$$D^2u_1 - i\tilde{p} = 0, \quad u_1(0) = Du_1(1) = 0, \tag{2.10}$$

where \tilde{p} is a real constant representing the pressure in the film. Like Poiseuille flow in a channel, this equation represents a balance between the normal-mode forms of the viscous-stress gradient D^2u_1 and the pressure gradient $-i\tilde{p}$. When \tilde{p} is positive, the pressure in the film is directly in phase with the surface deformation. Thus, the maximum pressure lies at the position of maximum interfacial deformation and decreases to each side. This pressure distribution drives a viscous flow that moves fluid away from the disturbance crests and towards the disturbance depressions, as shown in figure 5, producing a loss of mass under the crest and a decrease in the interfacial elevation. Thus, $\tilde{p} > 0$ represents a stabilizing effect on the film because the resulting longitudinal flow decreases the surface deformation.

We can now use this idea to predict the behaviour of the flow described by (2.7a). Here, there are three separate driving stresses for the shear flow. The first, $p_0 = \cot(\beta)$, is the extra hydrostatic pressure due to the displacement of the interface. Since it is positive, it pushes fluid away from the crest. It is a stabilizing effect.

The next two driving stresses arise from acceleration effects in the fluid and can be called inertial stresses. The first inertial stress, $R(\bar{u} - c_0)u_0$, is produced because of advection of the leading-order longitudinal velocity perturbation by the basic-state velocity relative to the moving disturbance. It is always negative because $u_0 > 0$ and $\bar{u} - c_0 < 0$ for $y \in (0, 1)$. Thus, it tends to push fluid underneath the crest and so it has a destabilizing effect on the film. The second inertial stress, $R\bar{u}'(-v_1)$, is produced because of the advection of the basic-state velocity by the leading-order normal velocity perturbation. It is also negative in the entire film and so it has a destabilizing effect.

The three driving stresses in (2.7a) produce the longitudinal flows shown in figures

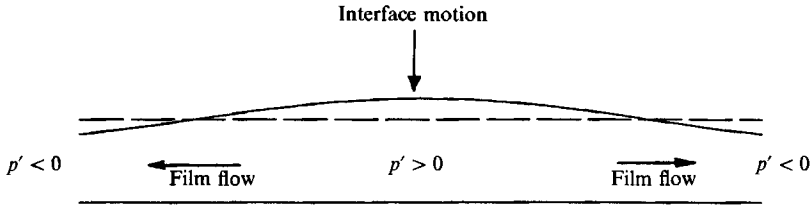


FIGURE 5. The direction of the disturbance film flow and the interfacial motion when a positive pressure lies underneath a disturbance crest. The long-dash line is the undisturbed free-surface position.

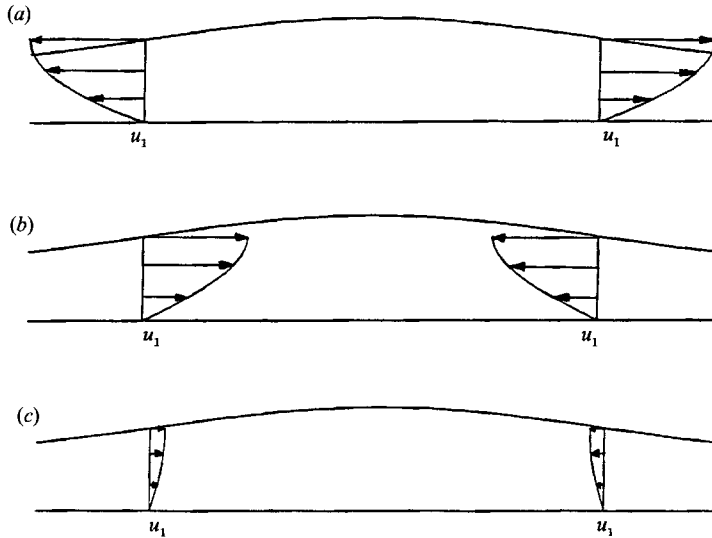


FIGURE 6. The first-order perturbation flows in a free-surface film owing to film stress for neutral conditions at $\beta = 45^\circ$. (a) The flow caused by the hydrostatic pressure under a disturbance crest, (b) the flow caused by the inertial stress due to the leading-order longitudinal velocity perturbation $R(\bar{u} - c_0)u_0$, and (c) the flow caused by the inertial stress due to the leading-order normal velocity perturbation $R\bar{u}'(-iv_1)$.

6(a-c). Each of these flows behaves exactly as we have predicted. These longitudinal flows in turn produce a normal motion of the interface given by

$$v_2(1) = -\frac{1}{3} \cot(\beta) + \frac{7}{60}R + \frac{1}{60}R. \tag{2.11}$$

Since $c_1 = v_2(1)$, we see that the first term represents the stabilizing effect of the normal component of gravity and the last two represent the destabilizing effect of the inertial stress associated with the leading-order longitudinal and normal velocity perturbations respectively. Note that the inertial stress due to the longitudinal velocity perturbation is seven times larger than that due to the normal velocity perturbation.

When the terms in (2.11) are arranged in another manner, we find

$$v_2(1) = -\frac{1}{3} \cot(\beta) + \frac{5}{24}R - \frac{3}{40}R. \tag{2.12}$$

Here, the second term represents the destabilizing effect of the inertial stress due to the advection of the leading-order longitudinal velocity perturbation by the motion of the disturbance at the phase speed c_0 . The third term is the net stabilizing effect of the inertial stresses due to advection associated with the basic-state velocity

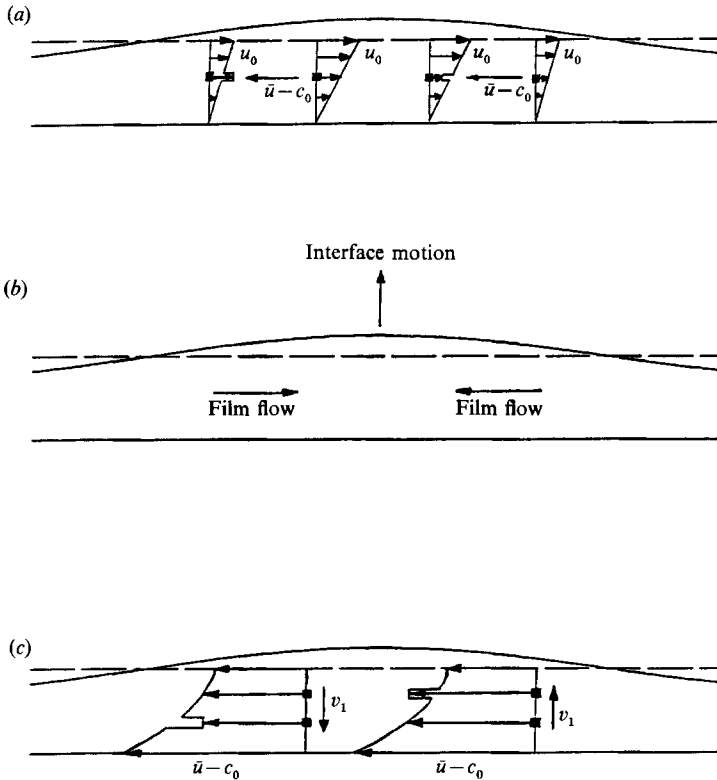


FIGURE 7. A schematic of the fluid advection interactions that produce the inertial stresses in a liquid film. (a) The advection of the leading-order longitudinal flow perturbation by the basic-state velocity relative to the moving disturbance to produce the negative inertial stress $R(\bar{u} - c_0)u_0$, (b) the film flow and the induced interfacial motion produced by the negative inertial stresses of both (a) and (c), and (c) the advection of the basic-state velocity by the leading-order normal flow perturbation to produce the negative inertial stress $R\bar{u}'(-iv_1)$. The long-dash line is the undisturbed free-surface position.

profile and the leading-order longitudinal and normal velocity perturbations. The unsteady effect of the wave motion dominates the effects of the convective acceleration terms. This is also true in the more general case of the film with an applied stress on its top surface. Thus, the unsteadiness associated with the moving disturbance is the dominant cause of the long-wave instability in this film.

A useful approximation to the behaviour of this system is the average driving stress for the film flow of (2.7a). If the average stress is positive (negative), we can estimate that the flow is stable (unstable). The average film stress is defined as

$$\tilde{p} = \int_0^1 \{p_0 + R(\bar{u} - c_0)u_0 + R\bar{u}'(-iv_1)\} dy. \tag{2.13}$$

For this system, we find

$$\tilde{p} = \cot(\beta) - \frac{7}{24}R - \frac{1}{24}R = \cot(\beta) - \frac{1}{3}R. \tag{2.14}$$

To estimate the critical Reynolds number, we set $\tilde{p} = 0$ and find $R_c = 3 \cot(\beta)$; a result 20% higher than the exact value of $R_c = \frac{5}{2} \cot(\beta)$.

Another way to understand the flows produced by the inertial stresses is to consider the acceleration effects of (2.7a) directly. Consider a coordinate system

moving with the phase speed of the disturbance so that the flow in the film is everywhere to the left. This flow interacts with the leading-order longitudinal velocity perturbation u_0 , shown in figure 3, and produces a negative inertial stress. In figure 7(a), we see a fluid particle just to the left of the crest and the associated perturbation flow profile, u_0 . The basic flow moves this particle to the left to a region where the perturbation flow is smaller. Thus, given what the disturbance expects to find at this location, the particle looks as if it has gained a velocity perturbation to the right, toward the crest. Likewise, to the right of the crest, the basic-state flow moves particles with a smaller longitudinal perturbation velocity to regions with a larger velocity. In this new location, the particle looks as if it has been given a velocity perturbation to the left, towards the crest. The resulting destabilizing flow is shown in figure 7(b), and it is exactly the same as the flow produced by the negative inertial stress.

The flow produced by the inertial stress associated with the leading-order normal perturbation velocity is described in a similar way. Here, we have a negative inertial stress produced through the interaction of $\bar{w}' > 0$ with $-iv_1 < 0$. In figure 7(c), we see that the normal perturbation velocity is upwards on the right-hand side of the crest and downwards on the left. On the right-hand side, the normal velocity moves fluid with a faster upstream basic-state velocity into a region with a smaller upstream velocity. The equivalent velocity perturbation for the fluid at this point is towards the crest. On the left-hand side of the crest, the downward normal velocity moves fluid with a slower upstream basic-state velocity into regions with a faster upstream velocity. The equivalent velocity perturbation will also be towards the crest. The net effect is again the destabilizing flow shown in figure 7(b).

3. Velocity-induced instability

The simplest fluid system that exhibits the velocity-induced long-wave instability is an isothermal liquid film flowing down a rigid inclined plane, but bounded above by a compliant surface. In a recent review, Riley, Gad-el-Hak & Metcalfe (1988) discussed the modelling of a compliant surface as a spring-backed, elastic plate with damping. We shall use the simplest such model in which the elastic plate has no mass, no bending stiffness, no damping, and it is not backed with springs. Thus, the upper compliant surface is just a thin elastic plate that moves parallel to the lower rigid plate at the velocity U_t . The geometry is shown in figure 1. We scale the velocity, length, time, and pressure as we did for the liquid film bounded by a gas and replace the tangential-stress boundary condition on the top surface by the no-slip condition. With these scalings, we obtain the dimensionless velocity of the compliant surface $U = U_t/U_s$ and must redefine the capillary number in terms of the longitudinal tension σ of the elastic plate.

The basic state is a steady, parallel shear flow given by

$$\bar{u} = \frac{1}{2}(y - y^2) + Uy, \quad \bar{p} = \cot(\beta)(1 - y), \tag{3.1 a, b}$$

$$\bar{v} = 0, \quad \bar{\eta} = 1. \tag{3.1 c, d}$$

The normal-mode disturbance equations for this model are given by system (2.2a-g), except that the boundary condition (2.2f) is replaced by the velocity boundary condition

$$\hat{u}(1) = -\bar{u}'(1)\hat{\eta}. \tag{3.2}$$

The ordered problems from the perturbation analysis for long waves on this system are as follows. At $O(1)$,

$$D^2 u_0 = 0, \quad u_0(0) = 0, \quad u_0(1) = \frac{1}{2} - U, \quad (3.3a, b, c)$$

$$u_0(y) = (\frac{1}{2} - U)y, \quad (3.3d)$$

$$Dp_0 = 0, \quad p_0(1) = \cot(\beta), \quad (3.4a, b)$$

$$p_0(y) = \cot(\beta). \quad (3.4c)$$

At $O(\alpha)$,

$$Dv_1 + iu_0 = 0, \quad v_1(0) = 0, \quad c_0 = \bar{u}(1) + iv_1(1), \quad (3.5a, b, c)$$

$$v_1(y) = -i\frac{1}{2}(\frac{1}{2} - U)y^2, \quad c_0 = \frac{1}{2}(U + \frac{1}{2}), \quad (3.5d, e)$$

$$D^2 u_1 = ip_0 + iR(\bar{u} - c_0)u_0 + R\bar{u}'v_1, \quad (3.6a)$$

$$u_1(0) = 0, \quad u_1(1) = 0, \quad (3.6b, c)$$

$$u_1(y) = i\cot(\beta)\frac{1}{2}(y^2 - y) + iR\frac{1}{12}\{U^2 - \frac{1}{4}\}\{-\frac{1}{2}y^4 + y^3 - \frac{1}{2}y\}. \quad (3.6d)$$

And at $O(\alpha^2)$,

$$Dv_2 + iu_1 = 0, \quad v_2(0) = 0, \quad c_1 = iv_2(1), \quad (3.7a, b, c)$$

$$v_2(y) = \cot(\beta)\frac{1}{2}\{\frac{1}{3}y^3 - \frac{1}{2}y^2\} + R\frac{1}{12}\{U^2 - \frac{1}{4}\}\{-\frac{1}{10}y^5 + \frac{1}{4}y^4 - \frac{1}{4}y^2\}, \quad (3.7d)$$

$$c_1 = i\frac{1}{12}\{-\cot(\beta) + R\frac{1}{40}(1 - 4U^2)\}. \quad (3.7e)$$

The critical Reynolds number is

$$R_c = \frac{40 \cot(\beta)}{1 - 4U^2}. \quad (3.8)$$

Note that the flow has a long-wave instability only when the phase speed of the disturbance is not contained in the range of \bar{u} .

For simplicity in the following discussion, we shall set $U = 0$. But again, the ideas presented are applicable to the more general case of non-zero U .

The only fundamental difference between the mechanism for this velocity-induced instability and that of the stress-induced instability studied in the previous section is the initiating mechanism. In figure 8, we see that when the interface is deflected by a disturbance, the basic-state will have a velocity at the new interface position that is different from the true interfacial velocity. This velocity is in the x -direction and it is equal to $\bar{u}'(1)\eta'$. Since the interface is a no-slip surface, a perturbation velocity develops at the undisturbed interface position that exactly cancels the velocity due to the basic state, as shown in (3.2). This perturbation velocity drives a longitudinal flow underneath the disturbance crest that is linear and varies directly with the displacement of the interface as shown in figure 3. Thus, the energy for the disturbance flow comes from the work done by the perturbation velocity at the compliant surface. To leading order, this work is exactly balanced by viscous dissipation in the film. Hinch (1984) described a version of this initiating mechanism for the case of an interface between two immiscible fluids as did Goussis & Kelly (1988).

The establishment of the leader-order longitudinal flow is the end result of the separate initiating mechanism for this model. After this point, the motion in the film is governed by the same processes as the instability in the film flow bounded above by a gas.

Following the control-volume argument given in the previous section (see figure 4), we see that the surface disturbance moves downstream relative to the interface. In fact, the phase speed $c_0 = \frac{1}{4}$ and so the disturbance moves faster than any fluid

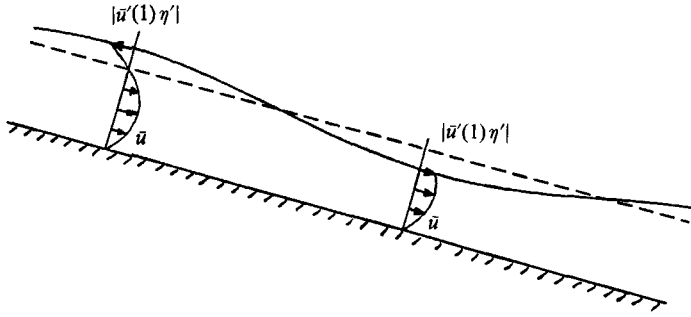


FIGURE 8. The development of an interfacial perturbation velocity owing to a disturbance on a film with a stationary compliant top surface.

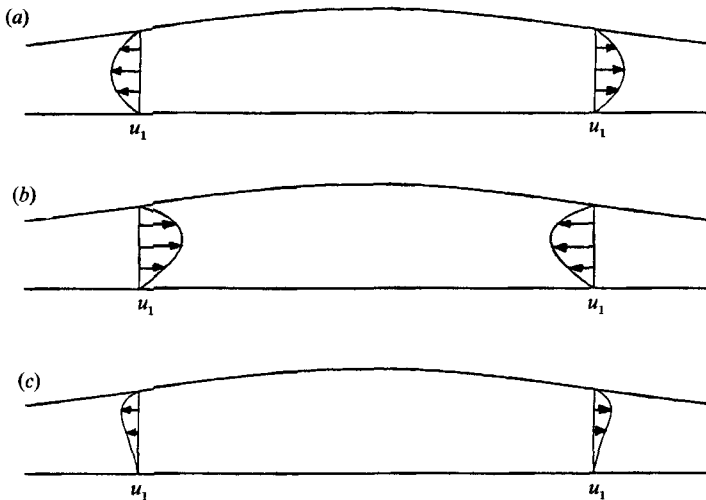


FIGURE 9. The first-order perturbation flows in a film with a stationary compliant top surface owing to film stress for neutral conditions at $\beta = 45^\circ$. (a) The flow caused by the hydrostatic pressure under a disturbance crest, (b) the flow caused by the inertial stress due to the leading-order longitudinal velocity perturbation $R(\bar{u} - c_0)u_0$, and (c) the flow caused by the inertial stress due to the leading-order normal velocity perturbation $R\bar{u}'(-iv_1)$.

particle in the film, the fastest of which is $\bar{u}(\frac{1}{2}) = \frac{1}{3}$. This behaviour is the same as that of the free-surface film.

In system (3.6a-c), we see that the growth mechanism of the instability involves a film flow similar to the one found for the free-surface film. The only difference is a rigid versus a free top surface. The first driving stress in the film is again $p_0 = \cot(\beta)$, the stabilizing hydrostatic pressure due to the displacement of the top surface and the component of gravity normal to the film.

The inertial stress produced by the advection of the leading-order longitudinal velocity perturbation by the basic-state velocity relative to the moving disturbance, $R(\bar{u} - c_0)u_0$, is always negative because $u_0 > 0$ and $\bar{u} - c_0 < 0$ for $y \in (0, 1)$. Thus, it is a destabilizing effect. The inertial stress produced by the advection of the basic-state velocity by the leading-order normal velocity perturbation, $R\bar{u}'(-iv_1)$, is negative in the lower half of the film and positive in the upper half because of the change in sign of $\bar{u}' = \frac{1}{2}(1-2y)$. Since $|-iv_1|$ is larger in the upper half of the film, this inertial stress has a net stabilizing effect.

These three stresses produce the longitudinal flows shown in figure 9. These flows in turn produce a normal motion of the interface given by

$$v_2(1) = -\frac{1}{12} \cot(\beta) + \frac{1}{320} R - \frac{1}{960} R. \quad (3.9)$$

Since $c_1 = v_2(1)$, we see that the first term represents the stabilizing effect of gravity, the second term represents the destabilizing effect of the inertial stress associated with the leading-order longitudinal velocity perturbation, and the last term represents the stabilizing effect of the inertial stress associated with the leading-order normal velocity perturbation.

A rearrangement of the terms in (3.9) yields

$$v_2(1) = -\frac{1}{12} \cot(\beta) + \frac{1}{192} R - \frac{1}{320} R. \quad (3.10)$$

Here, the second term represents the destabilizing effect of the inertial stress due to the advection of the leading-order longitudinal velocity perturbation by the motion of the disturbance at the phase speed c_0 . The third term is the net stabilizing effect of the inertial stresses due to advection associated with the basic-state velocity profile and the leading-order longitudinal and normal velocity perturbations. The unsteady effect of the wave motion dominates the effects of the convective acceleration terms. This is also true in the more general case in which the compliant top surface of the film is given a non-zero velocity. Thus, the unsteadiness associated with the moving disturbance is the dominant cause of the long-wave instability in this film.

The average film stress for this flow is

$$\tilde{p} = \cot(\beta) - \frac{1}{24} R + \frac{1}{48} R = \cot(\beta) - \frac{1}{48} R. \quad (3.11)$$

The critical Reynolds number from this approximation is $R_c = 48 \cot(\beta)$; a result 20% higher than the exact value of $R_c = 40 \cot(\beta)$.

4. Uniform-flow instability

The discussion in the previous two sections was primarily concerned with the details of the long-wave instability mechanism in thin liquid films. Now, we shall consider the instability mechanism in more general terms. The two film-flow models we have studied have several common features. In each model, (i) the interface is deformable normal to itself, (ii) the basic-state flow plus the leading-order perturbation flow behaves like a fully-developed viscous film flow driven by gravity and by the forcing of the top surface, (iii) the phase speed of an unstable long-wave disturbance is not contained in the range of the velocity in the undisturbed film, and (iv) unsteady inertial effects are the primary cause of the long-wave instability.

Using these observations we can describe the long-wave instability of liquid films in very simple terms. We shall confine ourselves to either a free film or a film with a stationary compliant top, but we note that these ideas are equally valid for the more general forced cases. Consider a disturbance to either of these liquid films in which the top surface is deflected upward slightly over a lengthscale that is much longer than the depth of the film. Because the height of the top surface varies slowly in the streamwise direction, the velocity profile at each streamwise location will approximate a fully-developed viscous film flow. For both of these films, it can be shown that the net longitudinal flow rate in the film is positive and that it increases with the depth of the film. Thus, at the crest of the deflection the longitudinal flow rate is a maximum and it decreases to each side. The net result of this is that gravity

draws fluid toward the front face of the crest, deflecting it upward, and gravity drains fluid from the rear face, deflecting it downward. This behaviour produces a forward motion of the disturbance without growth at a phase speed larger than the velocity of any fluid particle in the undisturbed film.

Now, at a particular instant in time, consider an x -location that is at the front face of a disturbance crest. Here, the surface height is increasing because of the forward motion of the disturbance. The flow in the bulk of the film is accelerating at this position because it is attempting to follow the fully-developed viscous velocity profile dictated by the surface height. However, inertial effects prevent the flow from accelerating fast enough to completely follow this velocity. The result is that the volume flux in the film is not as large as it should be if this was truly a fully-developed film flow. At the rear face of the crest, the velocity is decelerating, but inertial effects prevent the flow from decelerating completely enough. Thus, the volume flux in the film is larger than that due to a fully developed film flow. The net effect of these two volumes fluxes is an accumulation of fluid underneath the disturbance crest and an increase in the interfacial displacement. This is the destabilizing effect of the unsteady motion of the disturbance on the viscous film flow.

There are also convective acceleration effects in this flow that are stabilizing. On the front face of the crest, the flow is moving in a direction of decreasing surface height. As it does so, it must decelerate to follow the fully-developed viscous film flow. Inertial effects prevent the velocity from decelerating as completely as needed resulting in a flow slightly faster than expected for a fully-developed film flow. Similar arguments for the rear of the crest show that the longitudinal volume flux at this point is not as large as expected. The net result is a depletion of the fluid from under the disturbance crest. This is a stabilizing effect, but it is never larger than the destabilizing effect of the unsteady motion of the disturbance. Therefore, the overall effect of inertia is destabilizing.

The disturbance also produces an increase in the hydrostatic pressure under the crest proportional to the local depth of the film. This pressure tends to push fluid away from the disturbance crest resulting in a depletion of the fluid under the crest and a decrease in the depth of the film. This stabilizing flow competes with the inertial accumulation of fluid under the crest. If the inertial effect, as measured by the Reynolds number, is large enough, the film is unstable and the disturbance grows.

The long-wave instability mechanism described in this simple way can be displayed using a very simple flow model. Consider the liquid film on the inclined plane shown in figure 1, and model the flow of the liquid in this film with a uniform velocity profile. The flow is driven by the longitudinal component of gravity and by a longitudinal pressure gradient that is a result of the hydrostatic pressure produced by the long-wave deformation of the top surface and the normal component of gravity. We shall assume that some resistance to the flow occurs near the lower rigid boundary and at the upper surface, if it is compliant. This resistance takes the form of a shear stress that we model as being linear with respect to the longitudinal velocity of the liquid. Given this model, the following scaled equations of momentum and mass can be derived,

$$R\eta\{u_t + uu_x\} + u = \eta\{1 - \cot(\beta)\eta_x\} \tag{4.1}$$

$$0 = \eta_t + \{u\eta\}_x. \tag{4.2}$$

Here, u is the longitudinal velocity and η is the interfacial position. The parameter

R in the first equation is a Reynolds number for the flow measuring the relative importance of inertia to friction and $\cot(\beta)$ is a measure of the hydrostatic pressure gradient. Jeffreys (1925) used this same model, but with a shear stress on the inclined plane that was proportional to the velocity squared. Thus, he obtained the same equations, but with a u^2 instead of a u for the third term on the left-hand-side of (4.1).

The basic-state flow in this model is simply $\bar{u} = \bar{\eta} = 1$. A linear stability analysis of this flow produces the normal-mode disturbance equations

$$i\alpha R(\bar{u} - c)\hat{u} + \hat{u} = \hat{\eta} - i\alpha \cot(\beta)\hat{\eta}, \quad (4.3)$$

$$0 = i\alpha(\bar{u} - c)\hat{\eta} + i\alpha\hat{u}. \quad (4.4)$$

The long-wave approximation to the solution of these equations is

$$\hat{u} = 1 + i\alpha\{(c_0 - \bar{u})R - \cot(\beta)\} + \dots \quad (4.5)$$

$$c = c_0 + i\alpha\{(c_0 - \bar{u})R - \cot(\beta)\} + \dots \quad (4.6)$$

$$c_0 = 2, \quad \hat{\eta} = 1, \quad (4.7 a, b)$$

in which the last equation is a convenient normalization for the system. This film flow has a long-wave instability in which the critical Reynolds number is $R_c = \cot(\beta)$.

At the node point in front and at the back of a disturbance crest, $\eta' = 0$ and the disturbance velocity in the film is

$$u' = \mp \hat{u}_i \exp(\alpha c_i t), \quad (4.8)$$

where $\hat{u}_i = c_i = \alpha\{R - \cot(\beta)\}$. When the film is unstable, $R > \cot(\beta)$ and the disturbance flow in the film is to the left in front of the crest and to the right behind the crest. This leads to the accumulation of fluid under the crest and the disturbance grows.

The flow described by this simple model corresponds exactly to our description of the long-wave instability given at the beginning of this section. The basic-state flow plus the leading-order perturbation corresponds to a fully-developed flow in which the velocity is given by the local depth of the film. At the next order, the unsteady term produces a destabilizing longitudinal flow, the convective acceleration term produces a stabilizing longitudinal flow that is not as large as that produced by the unsteady term, and gravity produces a stabilizing longitudinal flow. We also see that the phase velocity of the disturbance is larger than the fluid velocity in the film.

The major features of the unstable flow in this simple model are also found in the previous models for a viscous film flow with either a free or a compliant upper surface. In addition, the only energy source for the disturbance in the uniform-flow model is the work done by the longitudinal body force on the disturbance. This is consistent with the disturbance energy analysis of Kelly *et al.* (1989), which shows that the energy for the disturbance in the viscous-flow models comes from the work done by perturbation surface shear stresses or surface velocities. These effects contain the details of the mechanism through which energy is pumped from the basic state to the disturbance. However, the energy in the basic state is there as a result of the work done by the longitudinal body force and the forces on the top surface. Thus, the detailed initiation mechanisms we described earlier are simply ways to describe how the longitudinal body force does additional work on the flow. This process is shown in a more transparent fashion in the uniform-flow model. These

results tell us that the uniform-flow model has captured the essence of the long-wave instability in thin liquid films.

5. Conclusions

We have described a physical mechanism for the long-wave instability that appears in thin liquid films. This mechanism gives a clear understanding of how a disturbance to the interface produces a motion in the film, and how this motion amplifies the disturbance. The complete detailed mechanism is composed of two parts; an initiating mechanism that produces the dominant motion in the film, and a growth mechanism that produces the unstable motion of the interface.

There are two different initiating mechanisms that can operate in liquid films, each one corresponding to a different type of boundary condition on the interface. The first mechanism is associated with the tangential-stress boundary condition on the interface. When the interface is deformed, a perturbation shear stress is induced such that the total interfacial shear stress at the undeformed interface position remains constant. The magnitude of this induced shear stress is proportional to the curvature of the basic-state velocity at the interface. The primary effect of the stress perturbation is to drive a longitudinal flow perturbation in the film and the work done by this stress is the main energy source for the instability. A liquid film on a rigid inclined plane bounded above by a free surface is the simplest system that exhibits this kind of behaviour.

The second mechanism is associated with the tangential-velocity boundary condition on the interface. When the interface is deformed, a tangential-velocity perturbation is induced at the undeformed interface position such that the total tangential velocity remains fixed. The magnitude of the induced velocity is proportional to the gradient of the basic-state velocity at the interface. This perturbation velocity drives a longitudinal flow perturbation in the film and the work that it does at the interface is the main energy source for the instability. The simplest example of this mechanism occurs in a film on a rigid inclined plane bounded above by a thin elastic plate.

In film flows composed of more than one liquid layer, both mechanisms can be important. When each layer has a different density, a jump in the curvature of the basic-state velocity across the interface will occur and the stress-initiation mechanism will operate. Likewise, when the viscosity in each layer is different, a jump in the basic-state velocity gradient across the interface will occur and the velocity-initiation mechanism will operate. This kind of behaviour has been demonstrated by Goussis & Kelly (1988) using a disturbance energy analysis of a two-layer flow in an inclined channel.

The growth mechanism of the instability produces the unstable motion of the interface and it operates regardless of the method of initiation. The leading-order velocity perturbations produced by the initiating mechanism interact with the basic-state velocity relative to the moving disturbance to produce inertial stresses that are proportional to the Reynolds number. When an inertial stress is positive, it drives a first-order flow perturbation that is away from disturbance crests and toward disturbance troughs. Such a flow reduces the interfacial deformation and is stabilizing. When an inertial stress is negative, the opposite destabilizing flow occurs. In the two films discussed here, the dominant inertial stress, which is destabilizing, is always due to the interaction of the leading-order longitudinal perturbation flow with the unsteady motion of the disturbance. Therefore, the net inertial stress in the

film produces a destabilizing flow that competes against the stabilizing flow created by the hydrostatic pressure field associated with the deformed interface. When the Reynolds number is large enough, the destabilizing flow dominates and the system is unstable.

The inertial stresses used in the growth mechanism for this instability can be used to estimate a critical Reynolds number for the film flow. From the solution of the leading-order problem, we can calculate an average film stress in the entire film as shown in (2.13). Setting this equal to zero produces an estimate for the critical Reynolds number. For both of the model flows examined here, this estimate was 20% higher than the exact value.

We have also described the mechanism of the long-wave instability in terms of a fully-developed, viscous film flow. When the interface of a thin film is deflected, the longitudinal flow in the liquid tends to follow the parallel, fully-developed viscous velocity profile dictated by the surface height. The first effect of this behaviour is a wave motion of the disturbance crest to the right since fluid is being drained from the left-hand side of the crest and pushed to the right. As this disturbance moves downstream, the flow in the film tries to stay in phase with the surface deflection. However, unsteady inertial effects prevent this and produce a flow with a phase lag behind the interfacial disturbance. The net result is an accumulation of fluid underneath the disturbance crest that increases the height of the disturbance. If the inertial effects are larger than the stabilizing effect of the normal component of gravity, the film is unstable. This mechanism for the long-wave instability is displayed very clearly in the uniform-flow model for the liquid film.

It is possible to extend the long-wave mechanism described in this paper to include flows of two or more layers bounded by rigid surfaces. This has been done by Smith (1989) for the stress-initiation mechanism in his study of a concentric two-phase flow in a vertical pipe. The extension lies in recognizing the existence of a large lubrication pressure that appears owing to the presence of the rigid boundaries. It is this lubrication pressure that accounts for the complicated behaviour of these systems as the geometry and stratification changes as shown by Smith (1989) and Renardy (1987*b*).

These same arguments can also be applied to the two-layer Couette flow first studied by Yih (1967), in which each layer has a different viscosity. This would be the simplest system that exhibits the velocity-induced instability and that includes the additional effects of the lubrication pressure.

This work was supported by the National Science Foundation, Grant no. MSM-8451093. The figures in this paper were drawn with the help of the NCAR plotting programs. The author would like to thank Professor Robert E. Kelly for a preprint of the paper Kelly, Goussis, Lin, & Hsu (1989) and Goussis & Kelly (1988). The arguments presented in this paper were greatly improved by the comments of the referees.

REFERENCES

- AKHTARUZZAMAN, A. K. M., WANG, C. K. & LIN, S. P. 1978 *J. Appl. Mech.* **45**, 25.
 BENJAMIN, T. B. 1957 *J. Fluid Mech.* **2**, 554.
 BINNIE, A. M. 1957 *J. Fluid Mech.* **2**, 551.
 GOUSSIS, D. A. & KELLY, R. E. 1985 *APS Bull.* **30**, 1732.
 GOUSSIS, D. A. & KELLY, R. E. 1988 *Phys. Fluids* (submitted).
 HICKOX, C. E. 1971 *Phys. Fluids* **14**, 251.

- HINCH, E. J. 1984 *J. Fluid Mech.* **144**, 463.
- HOOPER, A. P. 1985 *Phys. Fluids* **28**, 1613.
- HOOPER, A. P. & BOYD, W. G. C. 1983 *J. Fluid Mech.* **128**, 507.
- JEFFREYS, H. 1925 *Phil. Mag.* **49**, 793.
- JOSEPH, D. D., RENARDY, M. & RENARDY, Y. 1984 *J. Fluid Mech.* **141**, 309.
- KAO, T. W. 1965*a* *Phys. Fluids* **8**, 812.
- KAO, T. W. 1965*b* *Phys. Fluids* **8**, 2190.
- KAO, T. W. 1968 *J. Fluid Mech.* **33**, 561.
- KELLY, R. E., GOUSSIS, D. A., LIN, S. P. & HSU, F. K. 1989 *Phys. Fluids* **A1**, 819.
- LIN, S. P. 1975 *Lett. Heat Mass Trans.* **2**, 361.
- LISTER, J. R. 1987 *J. Fluid Mech.* **175**, 413.
- RENARDY, Y. 1987*a* *Phys. Fluids* **30**, 1627.
- RENARDY, Y. 1987*b* *Phys. Fluids* **30**, 1638.
- RILEY, J. J., GAD-EL-HAK, M. & METCALFE, R. W. 1988 *Ann. Rev. Fluid Mech.* **20**, 393.
- SMITH, M. K. 1989 *Phys. Fluids* **A1**, 494.
- SMITH, M. K. & DAVIS, S. H. 1982 *J. Fluid Mech.* **121**, 187.
- THAN, P. T., ROSSO, F. & JOSEPH, D. D. 1987 *Intl J. Engng Sci.* **40**, 70.
- WANG, C. K., SEABORG, J. J. & LIN, S. P. 1978 *Phys. Fluids* **21**, 1669.
- YIH, C.-S. 1963 *Phys. Fluids* **6**, 321.
- YIH, C.-S. 1967 *J. Fluid Mech.* **27**, 337.